Mineralogical Magazine, August 2013, Vol. 77(6), pp. 2857–2866

Irinarassite $Ca_3Sn_2SiAl_2O_{12}$ – new garnet from the Upper Chegem Caldera, Northern Caucasus, Kabardino-Balkaria, Russia

I. O. Galuskina[1,*], E. V. Galuskin[1], K. Prusik[2], V. M. Gazeev[3], N. N. Pertsev[3] and P. Dzierżanowski[4]

[1] Faculty of Earth Sciences, Department of Geochemistry, Mineralogy and Petrography, University of Silesia, Będzińska 60, 41-200 Sosnowiec, Poland
[2] Institute of Materials Science, University of Silesia, 75 Pułku Piechoty 1A, 41-500 Chorzów, Poland
[3] Institute of Geology of Ore Deposits, Geochemistry, Mineralogy and Petrography (IGEM) RAS, Staromonetny 35, Moscow, Russia
[4] Institute of Geochemistry, Mineralogy and Petrology, Warsaw University, al. Żwirki i Wigury 93, 02-089 Warszawa, Poland

[*Received 8 April 2013; Accepted 11 July 2013; Associate Editor: F. Cámara*]

ABSTRACT

Irinarassite, $Ca_3Sn_2SiAl_2O_{12}$, a new mineral species of the garnet supergroup was discovered in metasomatically altered carbonate-silicate xenoliths in ignimbrites of the Upper Chegem Caldera, Northern Caucasus, Kabardino-Balkaria, Russia. It occurs as small zones and irregular spots in kimzeyite-kerimasite or rarely as single crystals not exceeding 10 μm in size, within complex pseudomorphs after zircon. Lakargiite, tazheranite, baddeleyite, kerimasite, kimzeyite, baghdadite and rarely magnesioferrite are associated with irinarassite in the pseudomorphs which are confined to larnite-cuspidine zones immediately adjoining the ignimbrite. Larnite, cuspidine, rondorfite, fluor- and hydroxylellestadite, fluorite and secondary minerals such as ettringite, hillebrandite and bultfonteinite are associated with irinarassite. Irinarassite is pale brown to yellow colour. The mineral is characterized by the absence of cleavage and by an irregular fracture. The calculated density is 4.3 g cm^{-1}. The mineral is isotropic with a calculated refractive index of 1.9. The empirical crystal chemical formula of irinarassite from the holotype specimen is as follows $(Ca_{2.965}Fe^{2+}_{0.035})_{\Sigma 3}(Sn_{1.016}Zr_{0.410}Ti_{0.262}Sb^{5+}_{0.237}Fe^{2+}_{0.035}U^{6+}_{0.017}Sc_{0.014}Hf_{0.006}Nb_{0.004})_{\Sigma 2.001}(Al_{1.386}Fe^{3+}_{0.804}Si_{0.446}Ti^{4+}_{0.364})_{\Sigma 3}O_{12}$. Electron backscatter diffraction patterns of irinarassite are fitted to the garnet model with a = 12.50(3) Å with excellent MAD (mean angular deviation) = 0.16º. The Raman spectrum of irinarassite is analogous to those of kerimasite and other Zr-Sn-garnets of the schorlomite and bitikleite groups.

Keywords: irinarassite, garnet supergroup, Sn, EBSD, Raman, tazheranite, metasomatic rocks, Upper-Chegem Caldera.

Introduction

Irinarassite, $Ca_3Sn_2Al_2SiO_{12}$, a new garnet belonging to the schorlomite group in the garnet supergroup (Grew *et al*., 2013). Irinarassite occurs in the contact zone of an altered carbonate-silicate xenolith in ignimbrites of the Upper Chegem Caldera in the Northern Caucasus, Republic of Kabardino-Balkaria, Russia. Carbonate-silicate xenoliths altered under sanidinite-facies conditions, exposed along the ridge between the mountain peaks of Lakargi and Vorlan, are the source of six new mineral species belonging to the garnet supergroup (Galuskina *et al*., 2010*a*,*b*,*c*, 2011, 2013). Four of these, namely, bitikleite $Ca_3SnSbAl_3O_{12}$, dzhuluite $Ca_3SnSbFe_3O_{12}$,

* E-mail: irina.galuskina@us.edu.pl
DOI: 10.1180/minmag.2013.077.6.11

usturite $Ca_3ZrSbFe_3O_{12}$, elbrusite $Ca_3Zr_{1.5}U_{0.5}Fe_3O_{12}$ belong to the bitikleite group (Si-free garnets; cation charge at the Z site equal to 9) and the remaining two, toturite $Ca_3Sn_2Fe_2SiO_{12}$ and irinarassite $Ca_3Sn_2Al_2SiO_{12}$, to the schorlomite group (tetrahedral site cation charge equal to 10) in the classification of Grew *et al*. (2013). Irinarassite (IMA2010-73) was approved by CNMNC IMA in January of 2011. To date, a synthetic analogue of irinarassite has not been synthesized; only its synthetic Ti-analogue $Ca_3Sn_2Al_2TiO_{12}$, is known (Yamane and Kawano, 2011). Synthetic complex solid solution andradite-toturite-irinarassite-morimotoite-schorlomite garnet with 26.26 wt.% SnO_2 and an approximate formula $(Ca_{2.92}Mg_{0.08})_{\Sigma3}(Sn_{1.03}Ti_{0.28}Fe^{3+}_{0.54}Fe^{2+}_{0.15})_{\Sigma2}(Si_{1.84}Al_{0.53}Fe^{3+}_{0.63})_{\Sigma3}O_{12}$ has been reported in association with cassiterite in tin-refining slag (Butler, 1978). Tin garnets are very rare in nature (Galuskina *et al*., 2010*c*); up to 5.81 wt.% of SnO_2 has been reported in andradite (McIver and Mihálik, 1975; Amthauer *et al*. 1979; Kononov *et al*., 1989; Chen *et al*. 1992).

The name of this new mineral species irinarassite is given in honour of Irina Teodorovna Rass, an active member of staff since 1962 at the Korzhinskii Laboratory of Metamorphism and Metasomatism, Institute of Geology of Ore Deposits, Petrography, Mineralogy and Geochemistry (IGEM), Russian Academy of Sciences in Moscow. She is a well known specialist in the petrology and geochemistry of alkaline-ultramafic-carbonatite complexes, lamproites and kimberlites, and metasomatic processes. The type material (registration number 4026/1) is deposited in the collections of the Fersman Mineralogical Museum of the Russian Academy of Sciences in Moscow.

Methods of investigation

The morphology and composition of the garnets were investigated using a Philips/FEI ESEM XL30/EDAX scanning electron microscope and a CAMECA SX100 electron-microprobe analyser (EMPA) at 15 kV and 40−50 nA and a beam diameter of 1 μm using natural and synthetic standards: wollastonite – Ca*K*α, Si*K*α; periclase – Mg*K*α; rhodonite – Mn*K*α; Cr_2O_3 – Cr*K*α; Sc – Sc*K*α; orthoclase – Al*K*α; Fe_2O_3 – Fe*K*α; CeP_5O_{14} – Ce*L*α; LaB_6 – La*L*α; zircon – Zr*L*α; cassiterite – Sn*L*α; rutile – Ti*K*α; ThO_2 – Th*M*α; Hf – Hf*M*α; Sb_2O_5 – Sb*L*α; Nb – Nb*L*α; V_2O_5 – V*K*α; vorlanite – U*M*α.

The small size (<10 μm) of the irinarassite crystals required the use of single-crystal electron backscatter diffraction (EBSD) analysis to determine structural parameters and symmetry. The EBSD patterns were collected using a HKL EBSD system (HKL Technology Inc., Oxford Instruments Group) on a JEOL JSM-6480 scanning electron microscope (Institute of Materials Science, University of Silesia) using an accelerating voltage of 30 kV. Thin sections used for electron microprobe analyses were re-polished using an Al_2O_3 suspension (20 nm particles). To minimize charging, specimens were coated with a carbon layer several tens of nanometers thick. The calibration of the EBSD system was carried out using a Si single-crystal at detector distances of 177 mm (normal working position) and 155 mm (camera retracted position). A Nordlys II camera with a resolution of 1344×1024 pixels was used. To improve the pattern quality, acquisition times between 300 and 3000 ms and frame averaging were used. Depending on the detector distance and pattern collection time, up to 30 frames were averaged. The *Channel5* software package (Oxford Instruments; Day and Trimby, 2004) was used for the interpretation of the EBSD patterns. For the 155 mm detector distance, only manual band detection was used as data reduction using the Hough transform was ineffective. For the 177 mm detector distance, manual- and Hough (maximum 125 resolution) band detection was applied. In the match, 54 reflectors and 7-11 bands were used. An optimization procedure applied to estimate the symmetry and cell parameter of garnet supergroup minerals was described in detail by Galuskina *et al*. (2010*c*). *PowderCell* for Windows version 2.4 (Kraus and Nolze, 1996) helped to calculate the theoretical powder XRD pattern of irinarassite using the model with the best mean angular deviation from EBSD data and cation occupancy from electron-microprobe data.

Raman spectra of single crystals of irinarassite and associated kerimsite were recorded using a Dilor XY spectrometer equipped with a 1800 line/mm grating monochromator, a Peltier-cooled charge-coupled device (CCD) detector (1024×256) and an Olympus BX40 confocal microscope. The incident laser excitation was provided by a water-cooled argon laser source operating at 514.5 nm. The power at the exit of a

100× objective lens varied from 30 to 50 mW. The Raman spectra were recorded in 0º geometry in the range of 100–4000 cm^{-1} Raman shift and with spectral resolution of 2.5 cm^{-1}. A collection time of 20 s and accumulation of five scans were chosen. The monochromator was calibrated using the Raman scattering line of a silicon plate (520.7 cm^{-1}).

Occurrence and description of mineral species

Irinarassite was detected in altered xenolith no.7 located 500 m from the Vorlan peak in the central part of the Upper Chegem Caldera. A schematic geological map of the caldera with the locations of xenoliths within ignimbrites in the area between Vorlan and Lakargi peaks is given in Gazeev *et al*. (2006) and Galuskin *et al*. (2009). Xenolith no.7 forms a body ~5 m across. This xenolith is the type locality of another garnet, namely, usturite $Ca_3ZrSbFe_3O_{12}$ (Galuskina *et al*., 2010*a*) and also of vorlanite $CaUO_4$ (Galuskin *et al*., 2011). The xenolith comprises a chegemite central zone and larnite-cuspidine marginal zone (Galuskin *et al*., 2009). Irinarassite is found in the complex mixture of minerals forming pseudomorphs after zircon ranging up to 200 μm in size. These pseudomorphs occur at the immediate contact of skarn with unaltered ignimbrite. The contact rock is represented by a thin endoskarn zone. Larnite, cuspidine, rondorfite, As-bearing fluor- and hydroxylellestadite are the main minerals of this zone. Fluorite, rankinite, wollas-

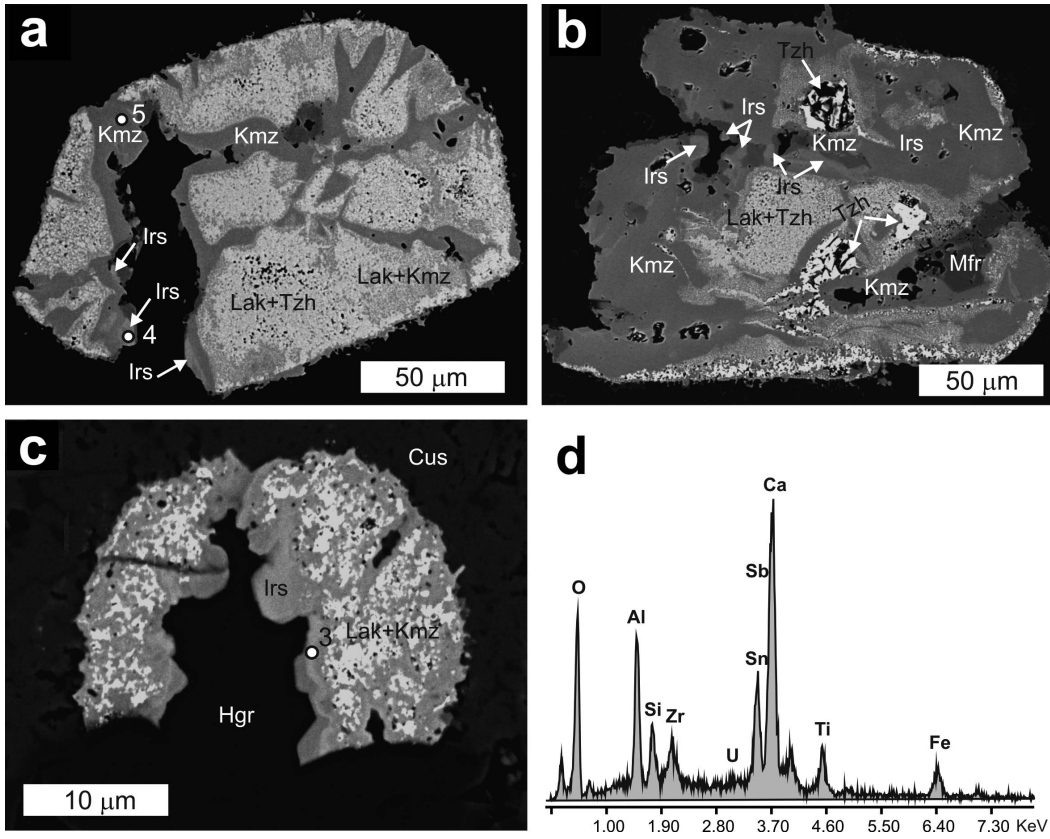

FIG. 1. (*a*,*b*) Complex pseudomorphs after zircon in which irinarassite occurs; 4, 5 – points of analyses in Table 1 where Raman spectra and EBSD patterns were obtained; (*c*) kimzeyite-lakargiite aggregate overgrown by garnet crystals with irinarassite zones, 3 – point of analysis in Table 1 where the EDS spectrum shown in Fig. 1*d* was obtained. Irs: irinarassite, Krm: kerimasite, Kmz: kimzeyite, Lak: lakargiite, Tzh: tazheranite, Mfr: magnesioferrite, Cus: cuspidine, Hgr: grossular-katoite.

tonite are minor minerals and secondary minerals are represented by minerals along the katoite-grossular join, ettringite, hillebrandite, bultfonteinite and unidentified Ca-hydrosilicates. As a rule, accessory minerals are represented by newly formed magnesioferrite, srebrodolskite, Th-bearing perovskite, lakargiite and relics of ignimbite minerals such as fluorapatite, titaniferous magnetite, thorianite and zircon. The pseudomorphs after zircon in which irinarassite was discovered commonly preserve the form of the original zircon (Fig. 1*a*). Garnet of the kerimasite–kimzeyite series, lakargiite and tazheranite are the main minerals in the pseudomorphs (Fig. 1*a*,*b*). Lakargiite and tazheranite are concentrated in the central zones of the pseudomorphs, whereas minerals of the schorlomite group develop on the periphery of the pseudomorphs or along radial cracks (Fig. 1*a*–*c*). Baddeleyite, baghdadite, magnesioferrite and zircon relics are relatively rare constituents of the pseudomorphs (Figs 1*a*,*b*; 2).

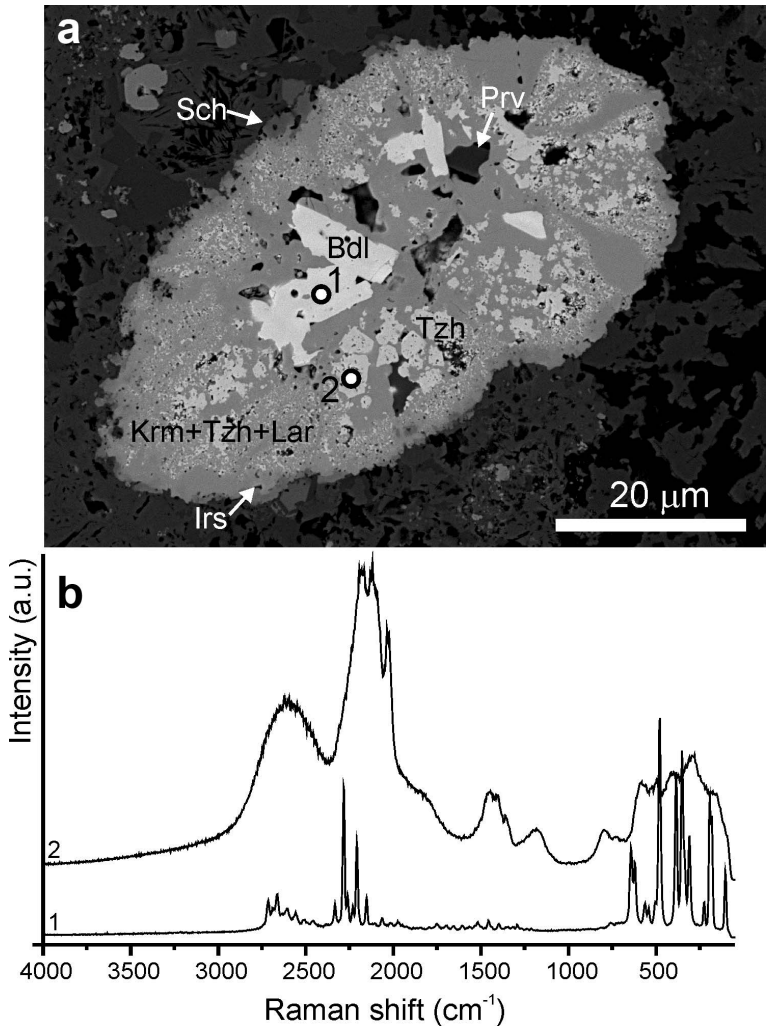

FIG. 2. (*a*) Rare example of a polymineralic pseudomorph after zircon with baddeleyite crystals. 1, 2 – points of Raman spectroscopy study. (*b*) Raman spectra of baddeleyite (1) and tazheranite (2). Bdl: baddeleyite, Tzh: tazheranite, Sch: schorlomite, Krm: kerimasite–kimzeyite solid solution, Lar: larnite, Prv: perovskite, Irs: irinarassite.

Irinarassite forms zones and irregular spots typically <10 μm in size in kerimasite–kimzeyite series minerals. In rare instances, the mineral occurs as crystals 2−3 μm in size (Fig. 1*a*−*c*). The colour of irinarassite varies from yellow to pale brown. The streak is ashy-yellow. The mineral does not show cleavage but exhibits irregular fracture. The density, calculated for the compositions of the mineral given in Table 1, is 4.301 and 4.260 g·cm^{-1} for analyses 1 and 2, respectively. The mineral is isotropic in thin-section. The calculated refractive index, using the Gladstone–Dale equation, is ~1.9 for analyses 1 and 2 (Table 1).

Irinarassite is a complex solid solution of garnet $Ca_3(Sn,Zr,Sb,Ti^{4+})_2(Al,Fe^{3+},Si,Ti^{4+})_3O_{12}$, which, according to the results of the Raman spectroscopy and EMPA investigations, does not contain significant amounts of OH or F (Table 1). Small amounts of UO_3, Nb_2O_5, HfO_2 or Sc_2O_3 are

TABLE 1. Chemical composition (wt.%) of irinarassite (1−4) and kerimasite (5) from the Upper Chegem Caldera.

	1			2			3	4	5
	Mean of 7	s.d.	Range	Mean of 6	s.d.	Range			
UO_3	0.76	0.07	0.66–0.85	0.27	0.06	0.17–0.33	0.85	0.66	0.16
Nb_2O_5	0.08	0.04	0–0.13	0.31	0.05	0.25–0.38	0.09	0.05	0.13
Sb_2O_5	5.99	0.56	5.42–6.81	7.85	1.34	5.22–8.81	5.48	6.02	5.21
SiO_2	4.19	0.16	3.92–4.45	4.16	0.30	3.89–4.73	4.16	4.17	4.68
TiO_2	7.82	0.39	7.28–8.34	7.02	0.33	6.62–7.59	8.14	8.01	5.61
ZrO_2	7.90	1.50	5.81–9.67	12.87	1.00	12.04–14.70	5.81	7.09	29.67
SnO_2	23.96	1.51	22.44–26.47	18.31	0.64	17.19–19.17	26.47	24.88	3.07
HfO_2	0.20	0.03	0.15–0.25	0.31	0.01	0.30–0.32	0.15	0.17	0.61
Al_2O_3	11.06	0.37	10.62–11.49	11.88	0.23	11.57–12.14	11.33	11.01	7.86
Sc_2O_3	0.15	0.11	0–0.32	0.16	0.04	0.09–0.20	n.d.	0.25	n.d.
Fe_2O_3	10.05	1.11	8.39–11.37	10.98	0.52	10.45–11.87	9.00	9.79	15.30
CaO	26.02	0.59	25.37–26.83	27	0.14	26.83–27.19	25.73	25.74	26.69
FeO	0.79	0.58	0–1.72	0.55	0.24	0.19–0.81	0.99	1.17	0.31
	98.96			101.67			98.20	99.00	99.30
Ca	2.965			2.967			2.961	2.937	2.993
Fe^{2+}	0.035			0.033			0.039	0.063	0.007
X	3.000			3.000			3.000	3.000	3.000
Sn^{4+}	1.016			0.749			1.133	1.056	0.128
Zr	0.410			0.644			0.304	0.368	1.514
Hf	0.006			0.009			0.005	0.005	0.018
Sb^{5+}	0.237			0.299			0.219	0.238	0.203
Nb^{5+}	0.004			0.014			0.004	0.002	0.006
U^{6+}	0.017			0.006			0.019	0.015	0.004
Ti^{4+}	0.262			0.252			0.266	0.251	0.107
Sc	0.014			0.014				0.023	
Fe^{2+}	0.035			0.014			0.050	0.041	0.020
Y	2.001			2.000			2.000	2.000	2.000
Al	1.386			1.436			1.434	1.382	0.970
Fe^{3+}	0.804			0.847			0.727	0.784	1.205
Si	0.446			0.427			0.447	0.444	0.490
Ti^{4+}	0.364			0.290			0.392	0.390	0.335
Z	3.000			3.000			3.000	3.000	3.000
Sch	68.4%			65.4%			68.9%	67.8%	76.4%
Btk	27.4%			32.5%			26.1%	27%	21.6%
Grt	4.2%			2.1%			5%	5.2%	2%

Total of group endmembers: *Shr* − schorlomite, *Btk* − bitikleite, *Grt* – garnet.

present in irinarassite. The empirical crystal chemical formula from the holotype specimen is: $(Ca_{2.965}Fe^{2+}_{0.035})_{\Sigma 3}(Sn_{1.016}Zr_{0.410}Ti_{0.262}Sb^{5+}_{0.237}Fe^{2+}_{0.035}U^{6+}_{0.017}Sc_{0.014}Hf_{0.006}Nb_{0.004})_{\Sigma 2.001}(Al_{1.386}Fe^{3+}_{0.804}Si_{0.446}Ti^{4+}_{0.364})_{\Sigma 3}$ (Table 1, analysis 1). The maximum content of SnO_2 in irinarassite reaches 26.47 wt.%, which equates to 1.133 a.p.f.u. in the empirical crystal chemical formula: $(Ca_{2.961}Fe^{2+}_{0.039})_{\Sigma 3}(Sn_{1.133}Zr_{0.304}Ti_{0.266}Sb^{5+}_{0.219}Fe^{2+}_{0.050}U^{6+}_{0.016}Hf_{0.005}Nb_{0.004})_{\Sigma 2}(Al_{1.434}Fe^{3+}_{0.727}Si_{0.447}Ti^{4+}_{0.392})_{\Sigma 3}O_{12}$ (Table 1, analysis 3).

Tazheranite, discovered in skarns of the Tazheran Massif in 1966, is a rare mineral that occurs in high-temperature skarns and in meteorites (Konev *et al*., 1969; Ma and Rossman, 2008; Galuskina *et al*., 2010*c*). Sn and Sb impurities and a small Ti content are characteristic of tazheranite associated with irinarassite (Table 2), giving an approximate tazheranite crystal chemical formula $Ca_2Zr_7O_{16}$, whereas that from the type locality is described by the crystal chemical formula $Ca_2Zr_5Ti^{4+}_2O_{16}$ (Rastsvetaeva *et al*., 1998). Baddeleyite, a rare constituent of the zircon pseudomorphs, is 98 mole% ZrO_2 with HfO_2 <1% (Table 2). It is assumed that the cubic tazheranite and monoclinic baddeleyite are polymorphs of ZrO_2 and that the cubic structure of the tazheranite is stabilized by Ca and Ti impurities (Konev *et al*., 1969). As tazheranite and baddeleyite commonly participate in the formation of particular Zr-based natural ceramics with micron-sized grained aggregates, Raman spectroscopy is one of the more appropriate methods for defining different polytypes of ZrO_2 (Fig. 2). As bands above 600 cm^{-1} are absent in the Raman spectra of the tazheranite, (Fig. 2), tetragonal modification – calzirtite – is excluded (Rossel, 1982; Sekulić *et al*., 1997).

In Fig. 3, unpolarized Raman spectra of irinarassite and kerimasite in the region 100–1100 cm^{-1}, obtained at the point where the EPMA were performed (Table 1, analyses 4 and 5; Fig. 1*a*), supporting the following crystal chemical formulae: irinarassite – $(Ca_{2.937}Fe^{2+}_{0.063})_{\Sigma 3}(Sn_{1.056}Zr_{0.368}Ti^{4+}_{0.251}Sb^{5+}_{0.238}Fe^{2+}_{0.041}Sc_{0.023}U^{6+}_{0.015}Hf_{0.005}Nb^{5+}_{0.002})_{\Sigma 2}(Al_{1.382}Fe^{3+}_{0.784}Si_{0.444}Ti^{4+}_{0.390})_{\Sigma 3}O_{12}$; kerimasite – $(Ca_{2.993}Fe^{2+}_{0.007})_{\Sigma 3}(Zr_{1.514}Sb^{5+}_{0.203}Sn_{0.128}Ti^{4+}_{0.107}Fe^{2+}_{0.020}Hf_{0.018}Nb^{5+}_{0.006}U^{6+}_{0.004})_{\Sigma 2}(Fe^{3+}_{1.205}Al_{0.970}Si_{0.490}Ti^{4+}_{0.335})_{\Sigma 3}O_{12}$.

The Raman spectrum of irinarassite is analogous to the kerimasite spectrum (Fig. 3) and other Zr-Sn-garnets of the schorlomite and bitikleite groups (Galuskina *et al*., 2010*a*, 2013). Low intensities and broadening of bands related to symmetric stretching vibrations in the tetrahedron $[ZO_4]$ in the region 850–650 cm^{-1} are

TABLE 2. Chemical composition (wt.%) of tazheranite and baddeleyite associated with the Chegem irinarasite.

	Tazheranite					Baddeleyite	
	Mean of 16	s.d.		a.p.f.u. based on 1 cation	a.p.f.u. based on 16O	Mean of 3	a.p.f.u. based on 1 cation
UO_3	0.22	0.34	0–1.11	0.001	0.007	n.d.	
Nb_2O_5	0.15	0.20	0–0.66	0.001	0.011	n.d.	
Sb_2O_5	1.22	0.63	0.31–2.25	0.008	0.073	n.d.	
SiO_2	0.23	0.15	0.06–0.54	0.004	0.038	0.05	0.001
TiO_2	2.18	0.50	0.87–3.00	0.029	0.264	0.08	0.001
ZrO_2	80.25	2.08	76.49–84.87	0.703	6.315	98.88	0.982
SnO_2	1.85	1.17	0.68–4.37	0.013	0.119	n.d.	
HfO_2	1.43	0.29	1.12–2.02	0.007	0.066	1.36	0.008
ThO_2	0.04	0.09	0–0.34		0.002	n.d.	
Al_2O_3	0.05	0.07	0–0.28	0.001	0.010	n.d.	
Sc_2O_3	0.03	0.03	0–0.08		0.004	n.d.	
Cr_2O_3	0.04	0.05	0–0.16	0.001	0.005	n.d.	
Fe_2O_3	1.04	0.21	0.62–1.42	0.014	0.126	0.35	0.005
MgO	0.06	0.03	0.01–0.13	0.002	0.015	n.d.	
CaO	11.16	0.47	10.29–12.05	0.215	1.929	0.13	0.003
Total	99.95					100.85	

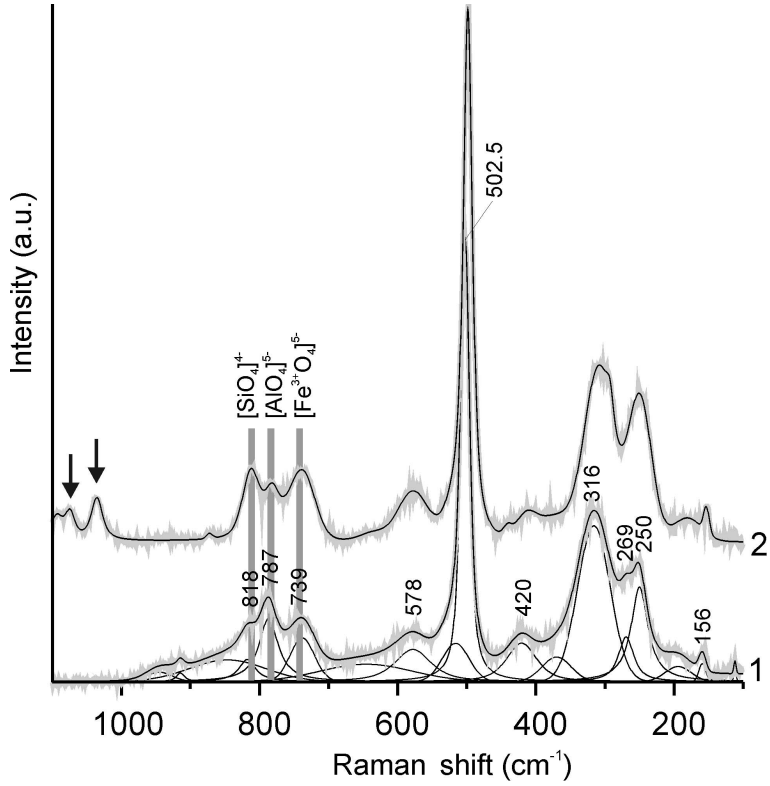

FIG. 3. Raman spectra of irinarassite (1) and kerimasite (2); the vertical arrows indicate bands from tazheranite.

characteristic of these spectra. This is connected with the fact that this position is occupied by cations with different ionic radii (Fe, Ti, Al), and for which the bands of $[Fe^{3+}O_4]^{5-}$ are at 730–750 cm^{-1}, from $[AlO_4]^{5-}$ are at 800–780 cm^{-1} and from $[SiO_4]^{4-}$ are >800 cm^{-1}. Broadening of bands also arises due to vibrations in $[TiO_4]^{4-}$, the bands from which lie between those from $[Fe^{3+}O_4]^{5-}$ and $[AlO_4]^{5-}$ in spectra. The appearance of the band near 580–600 cm^{-1} is caused by asymmetric stretching vibrations in $[Fe^{3+}O_4]^{5-}$ (Rulmont *et al*., 1995). In ^{Z}Al-dominant irinarssite, the 787 cm^{-1} band related to stretching vibrations in $[AlO_4]^{5-}$ has the greatest intensity in the region 850–650 cm^{-1}, whereas on the spectrum of $^{Z}Fe^{3+}$-dominant kerimasite this band has a relatively low intensity in comparison with bands from stretching vibrations in $[Fe^{3+}O_4]^{5-}$ and $[SiO_4]^{4-}$ (Fig. 3). The strong band near 500 cm^{-1} corresponding to bending vibrations in $[ZO_4]$ has a large half-width, reflecting the contribution of tetrahedra occupied by different cations (Al, Si and Fe^{3+}) in these types of vibrations (Fig. 3). Bands ~300 cm^{-1} are related to $[R(ZO_4)]$ whereas the band below 300 cm^{-1} is determined by translation motions of $T(ZO_4)$ and T(Ca).

Structural data for irinarassite were obtained using EBSD (Fig. 4) and fitting data according to modelling on the basis of the kimzeyite structure [ionic radii of ^{VI}Zr (0.72 Å) and ^{VI}Sn (0.69 Å) are similar (Shannon, 1976)], the space group $Ia\bar{3}d$ of the toturite structure [$a \approx 12.55$ Å] (Galuskina *et al*., 2010*c*) and the calculated a parameter for irinarassite analysis no. 1 (Table 1) on the formula (Strocka *et al*., 1978): $a = b_1 + b_2r_X + b_3r_Y + b_5r_Xr_Y + b_6r_Xr_Z + b_4r_Z$ (Å), where $b_1 = 7.02954$; $b_2 = 3.31277$; $b_3 = 2.49398$; $b_4 = 3.34124$; $b_5 = -0.87758$; $b_6 = -1.38777$ and r_X, r_Y, r_Z are the weight-averaged effective ionic radii of the cations (Shannon, 1976). The EBSD patterns for irinarassite and associated kerimasite were obtained at working distances of 155 mm and 177 mm. Fitting of the 155 mm working distance EBSD pattern for a model garnet with $a = 12.50(3)$ Å results in

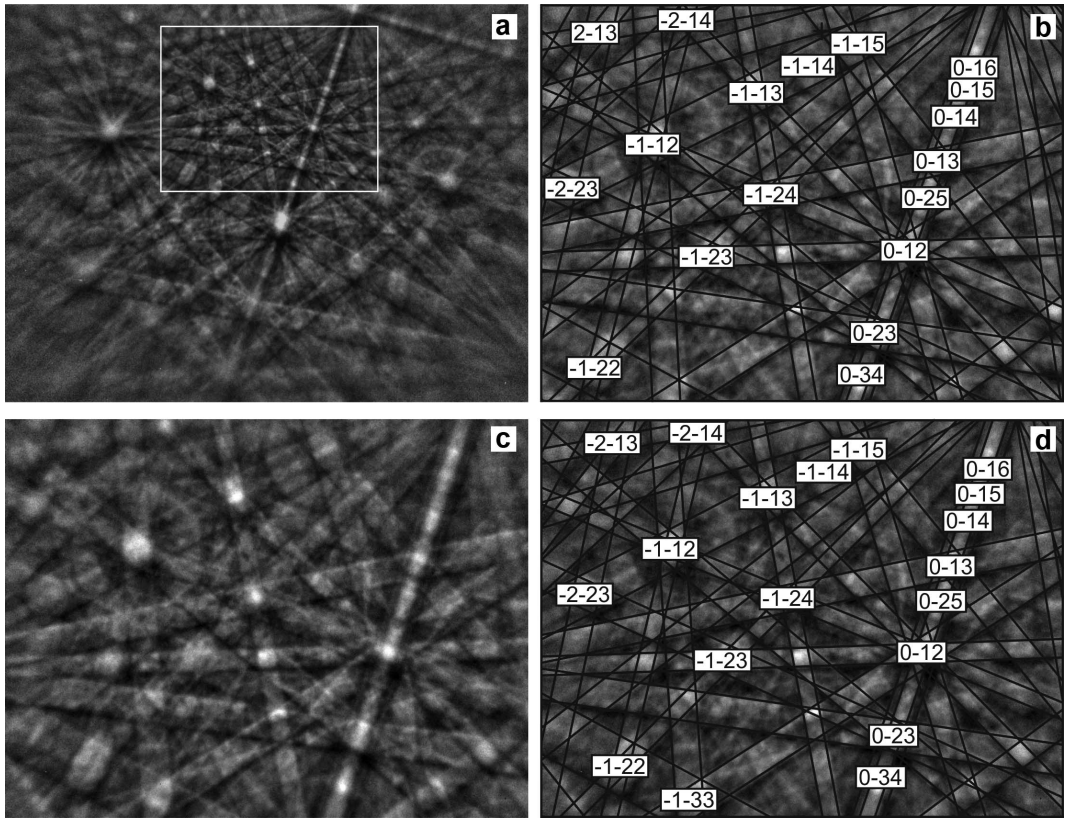

FIG. 4. EBSD patterns performed at separate zones of the garnet shown in Fig. 1*a* and fitting results to the garnet structure with a = 12.50 Å. (*a*, *b*) Kerimasite: (*a*) EBSD pattern for detector distances 177 and 155 mm (in inset), (*b*) fitting result for detector distance 155, MAD (mean angular deviation) = 0.24º; (*c*, *d*) irinarassite: (*c*) EBSD pattern for detector distance 155 mm, (*d*) fitting result, MAD = 0.16º.

values of the parameter MAD of 0.16º for irinarassite and 0.24º for kerimasite (excellent fitting). The calculated X-ray powder diffraction data are given in Table 3.

Discussion

Irinarassite, endmember $Ca_3Sn_2Al_2SiO_{12}$, is a complex solid solution containing components belonging to the schorlomite, bitikleite and garnet groups. The composition in Table 1 can be classified as the schorlomite group because cation charge at the *Z* site, 9.72−9.84, is close to the ideal value for this group (Grew *et al*., 2013). At the *Y* and *Z* sites of these garnets, four main cations are noted: Sn, Zr, Sb^{5+}, Ti^{4+} and Al, Fe^{3+}, Si, Ti^{4+}, respectively. Classification of these garnets should be carried out using the dominant-valency rule and taking double-site occupation into consideration (Hatert and Burke 2008). At the *Y* site, irinarassite has $R^{4+} > R^{5+} >>$ other cations, where Sn > Zr > Ti^{4+} (Table 1). There is valency-imposed double site-occupancy $(R^{4+}R^{3+})_2$ at the *Z* site, where Si > Ti for R^{4+}cations and Al > Fe^{3+} for R^{3+}cations.

Irinarassite $Ca_3Sn_2Al_2SiO_{12}$ is the fourth tin garnet discovered in altered xenoliths in ignimbrites of the Upper Chegem Caldera. It was found in xenolith no.7 (for numbering of xenoliths, see Galuskin *et al*., 2009). Toturite $Ca_3Sn_2Fe_2SiO_{12}$, the Fe^{3+}-analogue of irinarassite, is known from xenoliths no. 1 and 3, and bitikleite $Ca_3SnSb^{5+}Al_3O_{12}$ and dzhuluite $Ca_3SnSb^{5+}Fe_3^{3+}O_{12}$, minerals of the bitikleite group, were detected in xenolith no. 1. Irinarassite usually occurs as overgrowths on garnets of the kerimasite–

TABLE 3. Calculated XRD data for irinarassite (Co$K\alpha$ and Debye-Scherrer geometry).

h	k	l	d_{calc}	I_{calc}
2	2	0	4.4194	65
4	0	0	3.1250	60
4	2	0	2.7951	47
4	2	2	2.5516	88
5	1	0	2.4515	4
5	2	1	2.2822	4
4	4	0	2.2097	5
5	3	2	2.0278	6
6	2	0	1.9764	27
6	4	0	1.7334	16
6	4	2	1.6704	100
8	0	0	1.5625	22
8	2	2	1.4731	12
8	4	2	1.3639	14
7	6	1	1.3479	1
6	6	4	1.3325	26
8	5	1	1.3176	2
8	4	4	1.2758	6

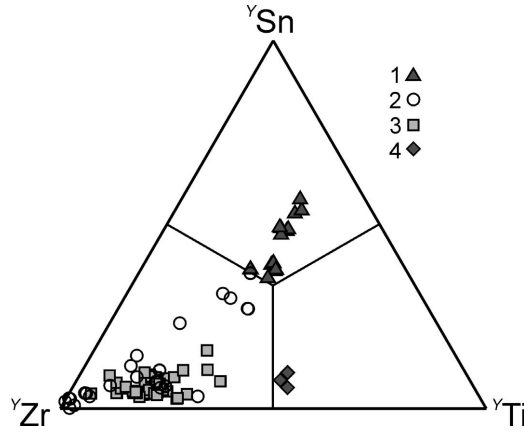

FIG. 5. *Y*-site occupancy in species of the schorlomite group. Symbols: 1 – irinarassite, 2 – kimzeyite, 3 – kerimasite, 4 – schorlomite.

kimzeyite series and, in rare cases, it forms zones in zirconian garnets (Fig. 1).

The following sequence of garnet crystallization from altered xenoliths in the Upper Chegem Caldera has been established previously as follows (Galuskina *et al*., 2013). The crystallization of the zirconian garnets, kerimasite and kimzeyite, was followed by that of the tin garnets, toturite and irinarassite. Garnets of the bitikleite group crystallized last in this sequence. In all cases, zirconian garnets are a substrate for the epitaxial crystallization of tin-, antimonian- and uranian garnets.

Investigation of garnet compositions associated with irinarassite show that there is continuous solid-solution between the zirconian- and tin garnets of the schorlomite group (Fig. 5). The simultaneous formation of Sn-garnets and a tazheranite-like phase in association with lakargiite, larnite, cuspidine, wadalite and rondorfite is indicative of skarn formation at unusually high temperatures (800–1000ºC). The formation of Sn-garnets in the area at the endocontact occurred under conditions involving intensive Si loss from the nearby ignimbrite towards the carbonate xenolith and remobilization of Zr from zircon to garnet and a ZrO_2-based phase. The source of the Sn is a more difficult question as Sn-bearing minerals have not been recognized in the ignimbrites. Melanocratic minerals such as micas, amphiboles and pyroxenes in which tin as a rule disperses during magmatic processes are the most likely source.

Acknowledgements

I.G. and E.G. acknowledge financial support by the Ministry of Science and Higher Education of Poland, grant no. N307 097038. The authors thank Pádhraig Kennan for English correction. The authors are grateful to Principal Editor Pete Williams and reviewers Edward Grew and Henrik Friis for their careful reviews which helped to improve the manuscript.

References

Amthauer, G., McIver, J.R. and Viljoen, E.A. (1979) ^{57}Fe and ^{119}Sn Mössbauer studies of natural tin-bearing garnets. *Physics and Chemistry of Minerals*, **4**, 235–244.

Butler, B.C.M. (1978) Tin-rich garnet, pyroxene and spinel from a slag. *Mineralogical Magazine*, **41**, 487–492.

Chen, J., Halls, C. and Stanley, C.J. (1992) Tin-bearing skarns of South China: Geological setting and mineralogy. *Ore Geology Reviews*, **7 (3)**, 225–248.

Day, A. and Trimby, P. (2004) *Channel 5 Manual HKL Technology Inc*., Hobro, Denmark.

Galuskin, E.V., Gazeev, V.M., Lazic, B., Armbruster, T., Galuskina, I.O., Zadov, A.E., Pertsev, N.N., Wrzalik, R., Dzierżanowski, P., Gurbanov, A.G. and Bzowska, G. (2009) Chegemite $Ca_7(SiO_4)_3(OH)_2$ –

a new humite-group calcium mineral from the Northern Caucasus, Kabardino-Balkaria, Russia. *European Journal of Mineralogy*, **21**, 1045–1059.

Galuskin, E.V., Armbruster, T., Galuskina, I.O., Lazic, B., Winiarski, A., Gazeev, V.M., Dzierżanowski, P., Zadov, A.E., Pertsev, N.N., Wrzalik, R., Gurbanov, A.G. and Janeczek, J. (2011) Vorlanite (CaU^{6+})O_4 – A new mineral from the Upper Chegem caldera, Kabardino-Balkaria, Northern Caucasus, Russia. *American Mineralogist*, **96**, 188–196.

Galuskina, I.O., Galuskin, E.V., Armbruster, T., Lazic, B., Dzierżanowski, P., Gazeev, V.M., Prusik, K., Pertsev, N.N., Winiarski, A., Zadov, A.E., Wrzalik, R. and Gurbanov, A.G. (2010*a*) Bitikleite-(SnAl) and bitikleite-(ZrFe) – new garnets from xenoliths of the Upper Chegem volcanic structure, Kabardino-Balkaria, Northern Caucasus, Russia. *American Mineralogist*, **95**, 959–967.

Galuskina, I.O., Galuskin, E.V., Armbruster, T., Lazic, B., Kusz, J., Dzierżanowski, P., Gazeev, V.M., Pertsev, N.N., Prusik, K., Zadov, A.E., Winiarski, A., Wrzalik, R. and Gurbanov, A.G. (2010*b*) Elbrusite-(Zr) – a new uranian garnet from the Upper Chegem caldera, Kabardino-Balkaria, Northern Caucasus, Russia. *American Mineralogist*, **95**, 1172–1181.

Galuskina, I.O., Galuskin, E.V., Dzierżanowski, P., Gazeev, V.M., Prusik, K., Pertsev, N.N., Winiarski, A., Zadov, A.E. and Wrzalik, R. (2010*c*) Toturite $Ca_3Sn_2Fe_2SiO_{12}$ – A new mineral species of the garnet group. *American Mineralogist*, **95**, 1305–1311.

Galuskina, I.O., Galuskin, E.V., Prusik, K., Gazeev, V.M., Pertsev, N.N. and Dzierżanowski, P. (2011) Irinarassite, IMA 2010- 073. CNMNC Newsletter No. 8, April 2011, page 292; *Mineralogical Magazine*, **75**, 289–294.

Galuskina, I.O., Galuskin, E.V., Kusz, J., Dzierżanowski, P., Prusik, K., Gazeev, V.M., Pertsev, N.N. and Dubrovinsky, L.S. (2013) Dzhuluite, $Ca_3SbSnFe_3^{3+}O_{12}$, a new bitikleite-group garnet from the Upper Chegem Caldera, Northern Caucasus, Kabardino-Balkaria, Russia. *European Journal of Mineralogy*, **25**, 231–239.

Gazeev, V.M., Zadov, A.E., Gurbanov, A.G., Pertsev, N.N., Mokhov, A.V. and Dokuchaev, A.Ya. (2006) Rare minerals from Verkhniechegemskaya caldera (in xenoliths of skarned limestone). *Vestnik Vladikavkazskogo Nauchnogo Centra*, **6**, 18–27 (in Russian).

Grew, E.S., Locock, A.J., Mills, S.J., Galuskina, I.O., Galuskin, E.V. and Hålenius, U. (2013) Nomenclature of the garnet supergroup. *American Mineralogist*, **98**, 785–811.

Hatert, F. and Burke, E.A.J. (2008) The IMA–CNMNC dominant-constituent rule revisited and extended. *The Canadian Mineralogist*, **46**, 717–728.

Konev, A.A., Ushchapovskaya, Z.F., Kashaev, A.A. and Lebedeva, V.S. (1969) Tazheranite – a new calcium-titanium-zirconian mineral. *Doklady Akademii Nauk SSSR*, **186**, 917–920 (in Russian).

Kononov, O.V., Evglevskaya, L.D., Klyuchareva, S.M., Korovkin, M.A. and Kabalov, Yu.K. (1989) Tin in garnet of the Tyrnyauz deposit. *Doklady Akademii Nauk SSSR*, **307**, 206–210 (in Russian).

Kraus, W. and Nolze, E. (1996) POWDER CELL – a program for the representation and manipulation of crystal structures and calculation of resulting X-ray powder patterns. *Journal of Applied Crystallography*, **29**, 301–303.

Ma, C. and Rossman, G.R. (2008) Discovery of tazheranite (cubic zirconia) in the Allende meteorite. *Geochimica et Cosmochimica Acta*, **72**, A577–A577.

McIver, J.R. and Mihálik, P. (1975) Stannian andradite from "Davib Ost," South West Africa. *The Canadian Mineralogist*, **13**, 217–221.

Rastsvetaeva, R.K., Pushcharovkiy, D.Yu., Spiridonov, E.M. and Gekimyants, V.M. (1998) Tazheranite and calzirtite: structural-mineralogical similarity and distinction. *Doklady Akademii Nauk*, **359**, 529–531 (in Russian).

Rossell, H.J. (1982) Calzirtite – a fluorite-related superstructure. *Acta Crystallographica*, **B38**, 593–595.

Rulmont, A., Tarte, P., Van Moer, A., Cartié, B. and Choisnet, J. (1995) Simultaneous occurrence of Sn^{4+} on the three cationic sites of the garnet structure: the solid solutions $Ca_xSn_xGa_{8-2x}O_{12}$ ($2.5 < x < 3.0$). *Journal of Solid State Chemistry*, **118**, 6–9.

Sekulić, A., Furić, K. and Stubičar, M. (1997) Raman study of phase transition in pure and alloyed zirconia induced by ball-milling and a laser beam. *Journal of Molecular Structure*, **410-411**, 275–279.

Shannon, R.D. (1976) Revised effective ionic radii and systematic studies of interatomic distances in halides and chalcogenides. *Acta Crystallographica*, **A32**, 751–767.

Strocka, B., Holst, P. and Tolksdorf, W. (1978) An empirical formula for the calculation of lattice constants of oxide garnets based on substituted yttrium- and gadolinium-iron garnets. *Philips Journal of Research*, **33**, 186–202.

Yamane, H. and Kawano, T. (2011) Preparation, crystal structure and photoluminescence of garnet-type calcium tin titanium aluminates. *Journal of Solid State Chemistry*, **184**, 965–970.